

POLYMER FLOW CONTROL IN CONTINUOUS GRAVIMETRIC BLENDERS

Alberto L. Cologni*
Simone Formentin[†]

Fabio Previdi
Dipartimento di Ingegneria
Università degli Studi di Bergamo
via Marconi 5, 24044 Dalmine (BG), Italy

Sergio M. Savaresi

Dipartimento di Elettronica, Informazione e Bioingegneria
Politecnico di Milano
Piazza Leonardo da Vinci 32, 20133 Milano, Italy

ABSTRACT

In this paper, the design of a plastic flow control system for continuous gravimetric blenders used in polymer extrusion processes is discussed. The considered plant is a blending machine that mixes four different polymers, bulks and additives. In order to pursue the desired behavior, three control objectives are considered: plastic flow estimation based on weight and screw speed measurements, plastic flow regulation for each meter and control of the recipe with mass constraints such that the mixer can always satisfy the plastic flow variation needed by the extruder. Simulation results are used to show the effectiveness of the proposed approach.

1 INTRODUCTION

Continuous gravimetric blenders are key elements in the plastic extrusion process, which has a standard setup including a feeding section, a barrel and a head with a die for shaping [1–3]. In the feeding section, the solid polymer is fed into the extruder through a blender in the form of granulate, pellets or irregular small bits. Usually, from two to six different polymeric components are blended in the feeding section by means of gravimetric or volumetric systems. Then, the polymer is transported along the barrel by means of a rotating screw. The barrel wall is equipped with a number of electric heaters which melt the polymer. The material is melted and pushed towards the die where the extruded final product is shaped and expelled. During the process, the polymer undergoes very complex thermo-mechanical transformations inducing strong changes in the physical properties of the material [4–6]. The final product quality in extrusion

is essentially characterized by a precisely-regulated volumetric flow of the polymer through the extruder [6–11]. This can be achieved by fine regulation of the mass flow delivered from the blender to the extruder.

Traditionally, continuous metering of plastic was performed by volumetric blenders, which are not equipped to measure the plastic quantity actually delivered to the extruder. So, they are controlled in open loop and their performance is limited. Recently, a new generation of plastic blenders for extrusion has been conceived, which are equipped with load cell to measure the plastic weight fed into the extruder. So, gravimetric blenders can provide accurate flow control by means of closed loop control [12]: they can give the chance of a considerable increase in performance, provided that an accurate mass flow estimate is computed on the basis of the weight measurements. In fact, in metering process, accuracy is an essential requirement in particular for additive components which are metered at very low flow values. Closed loop control of gravimetric blending provides many advantages with respect to volumetric blenders: metering is independent of material density variations; the frequent calibrations needed for volumetric feeders are not necessary; the increased accuracy considerably reduces the incidence of raw material costs, since each component is metered without any waste. In this paper, the control system design problem for a continuous gravimetric blender for four polymeric granulates is considered. Specifically, a multi-layer control architecture is employed, due to the peculiar structure of the plant dynamics. The inner loop is devoted to the regulation of the plastic flow of the primary meters. This control system is designed based on the estimation of the plastic flow obtained with an Extended Kalman Filter (EKF) [13]. Furthermore, the control algorithm is conceived such that the ratios among the components defined in the recipe

*Corresponding author. E-mail to: alberto.cologni@unibg.it

[†]Former PhD student at Politecnico di Milano.

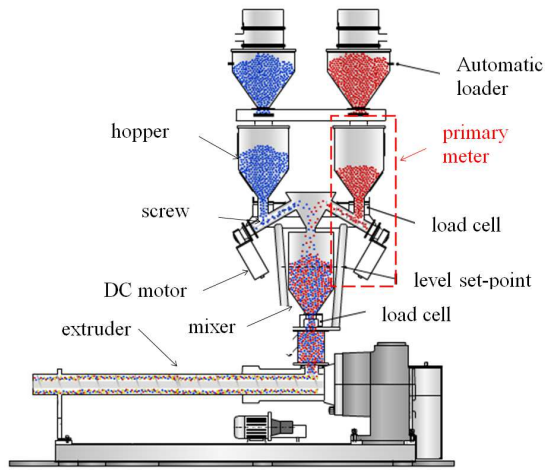


Figure 1: Schematics of the continuous gravimetric blender

are kept constant in every operating condition. The outer loop has the aim to keep a constant mass of plastic in the hopper directly connected to the extruder also during its flow variation requests.

The paper is organized as follows. In *Section 2*, the considered setup is illustrated and the control problems are defined. In *Section 3*, the global control architecture is described. In *Section 3.1*, the Extended Kalman Filter for plastic flow estimation is designed based on the mechanical model of the feeders. In *Section 3.2* and *Section 3.3*, the control algorithms for the primary meter and the mixer control loop for the recipe maintenance are described, respectively. The paper is ended by some concluding remarks.

2 CONTINUOUS GRAVIMETRIC BLENDERS

The mechanical layout of the continuous gravimetric blender considered in the present work is shown in Figure 1, where an example of two component blending (the blue and the red one) is considered. The device is made of two parts:

1. a set of primary meters (from one to six), devoted to supply the correct flow of each component, which must be delivered in fixed proportion according to the given recipe;
2. a secondary hopper (the mixer), where the various ingredient flows are mixed in a homogeneous blend with perfect additive dispersion. The mixed material is then fed to the extruder; it must be noticed that the extruder can draw different flow values of the mixed components, according to the extrusion throughput required by its own control system.

Each primary meter is made of three parts: a hopper, containing the component; a screw, that delivers the materials proportionally to its revolution speed; a DC motor actuating the screw through a 10x gear. So, changing the motor speed, it is possible to change the screw speed and, at last, the material flow. The primary meter operation is based on the loss-in-weight measure-

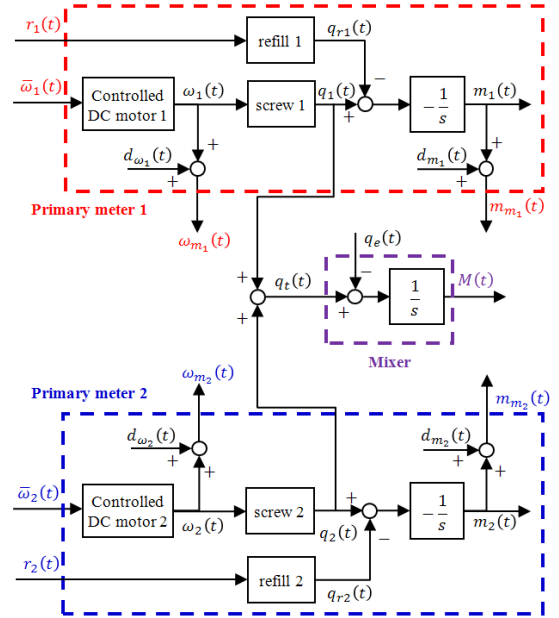


Figure 2: System theoretic representation of the considered plant

ment principle: the weight of the component hopper is measured in real-time; so, at least in principle, it is possible to compute the flow by weight measurement differentiation. Finally, since all the ingredient weights are continuously and simultaneously measured, it is expected that the total mass poured into the mixer is composed by the different ingredients in the correct ratios fixed by the recipe.

The mixer is endowed with a load cell that measures the mixer weight in order to prevent from undesired emptying; in fact, if the mixer does not contain enough material the blender could not be able to satisfy large flow variation requests from the extruder.

All the primary meters, when it is necessary, can be refilled with the opening of pneumatic valves, that allow the fall of the material from the automatic loaders.

A block diagram representation is shown in Figure 2 for a two components blender. The control variables are the reference speed $\bar{\omega}_1(t)$ and $\bar{\omega}_2(t)$ of the DC motors, which are endowed with a speed control loop. The measurements $\omega_{m_1}(t)$ and $\omega_{m_2}(t)$, respectively of the revolution speeds $\omega_1(t)$ and $\omega_2(t)$, are affected by quantization noises $d_{\omega_1}(t)$ and $d_{\omega_2}(t)$. The flow rates in output ($q_1(t)$ and $q_2(t)$) are collected into a mixer that is connected directly to the extruder.

In every meter, during the refill, the flow rates $q_1(t)$ and $q_2(t)$ are subtracted respectively with $q_{r1}(t)$ and $q_{r2}(t)$. These resulting exiting flows can be integrated in order to obtain $m_1(t)$ and $m_2(t)$; the real outputs $m_{m_1}(t)$ and $m_{m_2}(t)$ are defined as $m_1(t)$ and $m_2(t)$ affected by noises $d_{m_1}(t)$ and $d_{m_2}(t)$.

This plant has three main control objectives:

1. each primary meter must deliver the ingredient to the mixer with the highest possible accuracy;
2. all the primary meters must deliver the ingredients according

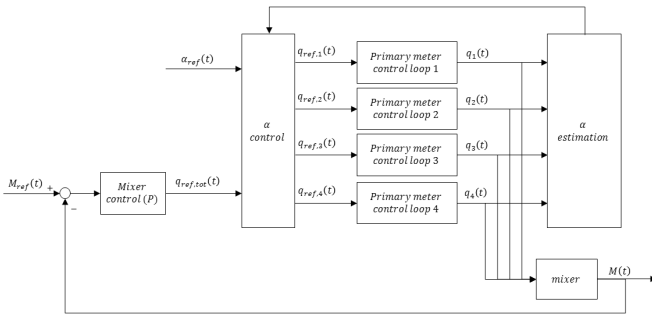


Figure 3: Control scheme

to the ratios defined by the recipe, in particular during flow changes following extruder requests;

3. the mixer must be able to provide all the requested plastic flow to the extruder, and therefore a maximum reduction of 1/3 of the maximum flow is allowed.

In the rest of the paper, a 4 component blender will be considered of the above described type.

3 CONTROL STRATEGY AND DESIGN

The multilayer control scheme depicted in Figure 3 is herein employed. For each primary meter, suitable closed loop control is devised. The inputs of each primary meter block are obtained from the recipe control: its main target is to guarantee the respect of the recipe during the flow rate transients also in presence of undesired behaviours of the meters (*i.e.* dynamic variations). The total required flow rate, incoming in the recipe control, is obtained through a third controller, made with the aims of guarantee the presence of material for the extruder and avoid undesired fills of the mixer. Notice that this structure of control allows one to use the same control algorithm in machines with any number of primary meters.

3.1 Extended Kalman Filtering

In order to obtain a flow rate estimation, for each meter, an extended Kalman filter is implemented based on the mechanical model of the feeders. Notice that such a filtering strategy is very suited for control design, see *e.g.* [14, 15].

As shown in Section 2, the primary meter is made of a speed controlled DC brushless motor connected to a speed reducer (reduction factor 10) that enables movement of a worm screw. The state space equations are

$$\begin{cases} \frac{dq_s(t)}{dt} = \frac{1}{\tau}(-q_s(t) + K_s(t)\omega(t)) \\ \frac{dm(t)}{dt} = -\alpha q_s(t) + K_r(t)r(t) \\ y(t) = m(t), \end{cases} \quad (1)$$

where:

- t is the temporal index
- $\omega(t)$ is the motor speed [rpm]
- $r(t)$ is the refill signal [0 – 1]
- $q_s(t)$ is the meter output flow rate [kg/h]
- $K_s(t)$ is the gain between the speed $\omega(t)$ and $q_s(t)$ [kg/h/rpm]
- τ is the time constant of the meter first order model [s]
- α is the fixed conversion from kg/h to kg/s ($\alpha = \frac{1}{3600}$)
- $K_r(t)$ represents the amount of material inserted in the hopper during the refill per time unit [kg/s]
- $y(t)$ represents the real output of the system

This model defines the flow rate $q_s(t)$ as a speed signal $\omega(t)$ multiplied by a variable gain $K_s(t)$. The mass variation into the hopper is defined as a balance of the flow rates: the incoming flow rate from the refill valve $K_r(t)r(t)$ and the outgoing $\alpha q_s(t)$. Notice that such a model is not time-invariant. The meter time constant τ is considered fixed to 1 s. The signal $K_s(t)$ is dependent on the density of the material, the design of the worm screw and, in extreme conditions (with $\omega(t)$ very closed to 0), from $\omega(t)$. The signal $K_r(t)$ is dependent from the density of the material, the design of the refill valve and from the quantity of material inside the automatic loader.

For these reasons and typically low signal-to-noise ratios, an extended Kalman filter, and not a simple derivator of the mass, is designed in order to obtain an accurate estimation of $q_s(t)$.

Consider the discretization of model (1):

$$\begin{cases} q_r(n+1) = K_r(n)r(n) \\ q_s(n+1) = \frac{1}{\tau + t_s/2}((\tau - t_s/2)q_s(n) + t_s K_s(n)\omega(n)) \\ m(n+1) = t_s(-\alpha q_s(n) + q_r(n)) + m(n) \\ y(n) = m(n) \end{cases} \quad (2)$$

where n is the temporal index and $q_r(n)$ is the refill flow rate [kg/s]. The model can be linearized assuming steady state inputs $r(n) = \bar{r}$ and $\omega(n) = \bar{\omega}$, thus obtaining state space model:

$$A = \begin{bmatrix} 0 & 0 & 0 \\ 0 & \frac{\tau - t_s/2}{\tau + t_s/2} & 0 \\ t_s & -\alpha t_s & 1 \end{bmatrix}, \quad B = \begin{bmatrix} \bar{k}_r & 0 \\ 0 & \frac{t_s \bar{k}_s}{\tau + t_s/2} \\ 0 & 0 \end{bmatrix}, \quad (3)$$

$$C = [0 \quad 0 \quad 1], \quad D = [0 \quad 0].$$

with:

$$\begin{cases} x(n+1) = Ax(n) + Bu(n) \\ y(n) = Cx(n) + Du(n) \end{cases} \quad (4)$$

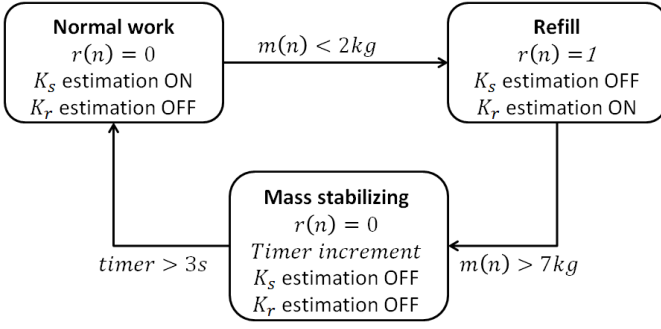


Figure 4: Machine-state of gains estimation

Defining state covariance matrix V_1 , output covariance matrix V_2 and supposing cross-correlation matrix $V_{12} = 0$, it is possible to obtain an *a priori* estimation error covariance matrix $P(n)$ according to the Differential Riccati Equation (DRE):

$$P(n+1) = A^+(n)P(n)A^+(n)^T + V_1 + (A^+(n)P(n)C^T)(CP(n)C^T + V_2)^{-1}(A^+(n)P(n)C^T)^T \quad (5)$$

where (referred to Equation (3)):

- $A^+(n)$ is the linearized state matrix A at sample n with the addition of K_r and K_s states (fifth order)
- C is the output matrix of the linearized model (constant)

The current Kalman gain matrix $K_K(n)$ can be computed as

$$K_K(n) = (A^+(n)P(n)C^T)(CP(n)C^T + V_2)^{-1} \quad (6)$$

The estimations \hat{K}_r , \hat{K}_s , \hat{q}_r , \hat{q}_s , \hat{m} are made through the implementation of the discrete model (2). The innovation term $e(n) = m(n) - \hat{m}(n)$, multiplied by matrix $K_K(n)$, is used as an additional input, which corrects the state estimate according to the current measurements.

In order to avoid large fluctuations of \hat{K}_r and \hat{K}_s (that are slowly time-varying) in the model implementation a machine-state is used (see Figure 4). During the normal working the refill valve is kept closed ($r(n) = 0$). In this case, the estimation of K_r is switched off. During the refill ($r(n) = 1$), the mass signal has a very large dynamic and a very big noise, for these reasons the estimation of K_r is switched on, while the estimation of K_s is turned off. At the end of the refill, it is necessary to wait for the weight stabilization (fixed to 3 seconds after the closing of the refill valve, due to mechanical vibrations of the hopper), during which the estimations are held off.

The validation of the filter is made through multiple tests on different screw layouts. In order to check all the extreme cases the smallest and the biggest screws are tested (theoretical gains: $K_s = 0.00698 \text{ kg/h/rpm}$ and $K_s = 0.119 \text{ kg/h/rpm}$, material: PP - density $\rho = 0.65 \text{ kg/dm}^3$).

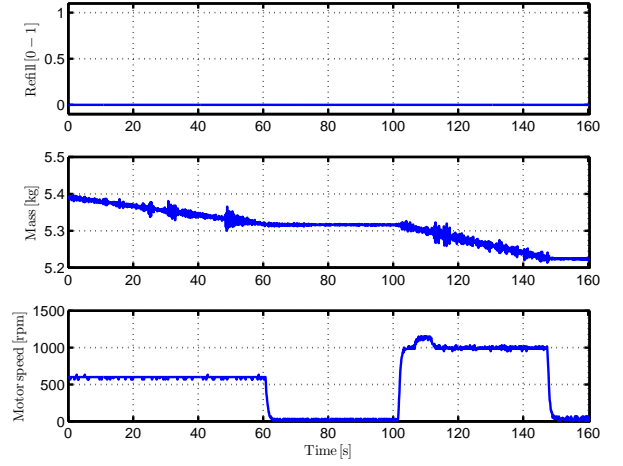


Figure 5: Input filter signals, small screw

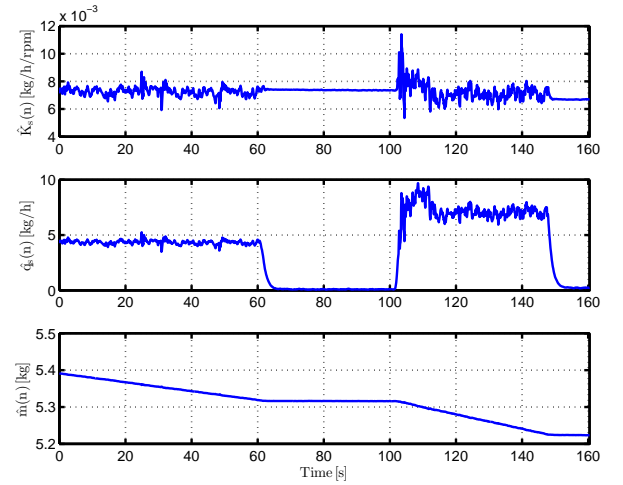


Figure 6: Estimated signals, small screw

As shown in Figure 5 the first experiment is made with a small screw and with a speed reference $\omega_{ref}(n)$; in this experiment, in which the filter is in steady state, the refill valve is always closed, for these reasons the estimations of K_r and q_r are not shown. The outputs of the EKF (in this experiment) are shown in Figure 6: the estimated variables are K_s , q_s and m .

In order to make a performance evaluation of the filter, starting from \hat{q}_s (the estimation of q_s) an estimated mass signal called \hat{m}_q is calculated as follows:

$$\hat{m}_q(n) = m_0 - \alpha t_s \sum_{i=0}^n \hat{q}_s(i), \quad (7)$$

where m_0 is assigned with the first sample $m(0)$. This signal is compared with the real mass signal m by calculating the error

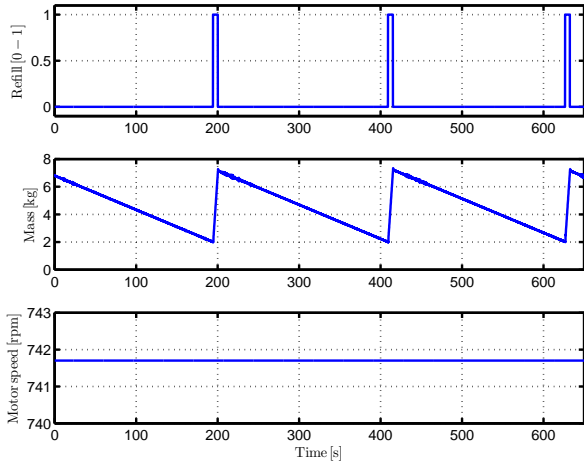


Figure 7: Input filter signals, large screw

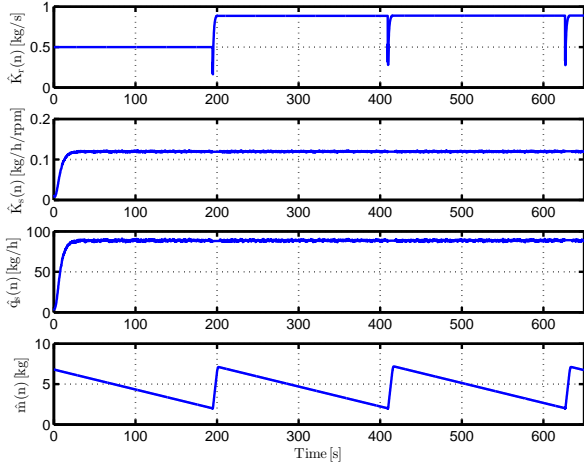


Figure 8: Estimated signals, large screw

$e_q(n) = m(n) - \hat{m}_q(n)$. The final error is 0.0018 kg against a quantity of metered material equal to 0.217 kg. The mean error in q_s estimation obtained in this experiment is then below 1 %.

In the second experiment, complete work cycles with the largest screw are executed. The speed reference $\omega_{ref}(n)$ is set as a constant value. As shown in Figure 7, in the experiment the refill valve is opened three times and, during these periods, the mass signal increases up to 7 kg. The estimated variables K_r , K_s , q_s and m are shown in Figure 8 (q_r is not plotted because it is defined as the product between $K_r(n)$ and $r(n)$). The settling time of the screw parameters K_s and q_s is approximately equal to 25 seconds and the K_r parameter reaches the real value during the first refill.

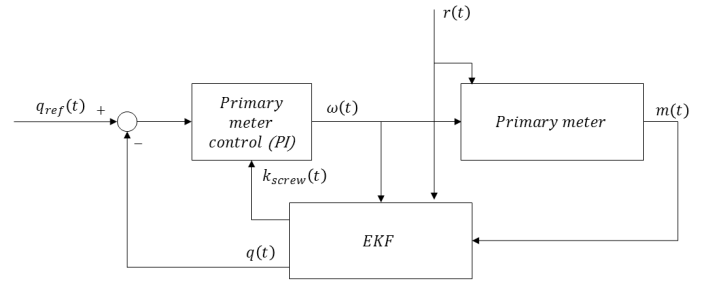


Figure 9: Primary meter control scheme

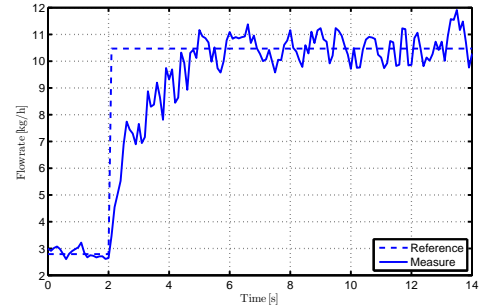


Figure 10: Primary meter closed loop step response, small screw

3.2 Primary meter control

Once a good estimation of q_s is obtained, it is possible to design a closed-loop system with the aim of guaranteeing, for each primary meter, a plastic flow rate close to the desired $q_{s,ref,i}$ (i represents the index of the meter from 1 to N). In Figure 9, it is clear how the estimated flow rate signal becomes the variable to control in this primary meter layer. The main objective of this control step is to achieve acceptable performance for all the screw/material couples (*i.e.* maximal transient time of 5 s).

The choice of a PI controller is performed by evaluating the transfer function of the linear tangent system from $\omega(t)$ to $q_s(t)$ when the estimated flow rate $\hat{q}_s(t)$ is supposed equal to $q_s(t)$, *i.e.* it is of first order. The PI proportional and integral gain, that is K_p and K_i , are obtained by pole placement technique.

As it can be observed in Figures 10 and 11, the control loop guarantees that the required performance is achieved and the settling time is always less than 5 seconds.

3.3 Recipe and mixer control

The primary meter control schemes need to be fed by a flow rate reference signal. The trajectory generation for such reference plastic flows are given by two outer control loops designed to respect the recipe and the mass constraints in the mixer. As a matter of fact, one of the main objectives of the dosing machine is to guarantee the achievement of the recipe against undesired behaviors of some primary meters. In order to avoid this problem an external control loop is designed: the machine user can

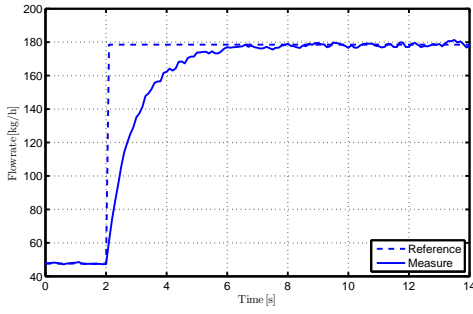


Figure 11: Primary meter closed loop step response, large screw

define the distribution (in terms of fractions $\alpha_{ref,i}$) of the flow rate on the different primary meters and the closed-loop system must ensure, in all conditions, its respect.

In order to define the architecture of this control system, the dosing machine with four primary meters described in Section 2 is considered. For primary meters, the actual flow rate fraction $\alpha_i(t)$ can be defined as follows:

$$\alpha_i(t) = \frac{q_{s,i}(t)}{\sum_{j=1}^N q_{s,j}(t)}, \quad \alpha_N(t) = 1 - \sum_{j=1}^N \alpha_j(t). \quad (8)$$

As described in Section 3.2, the estimated flow rate $\hat{q}_{s,j}$ is supposed equal to $q_{s,j}$. Starting from the total flow rate reference $q_{ref,tot}$, in order to guarantee that

$$q_{ref,tot}(t) = \sum_{i=1}^N q_{s,ref,i}(t), \quad (9)$$

the inputs of this outer system $p_i(t)$, $i = 1 \dots N - 1$ are included in each flow rate reference as

$$\begin{aligned} q_{s,ref,i}(t) &= q_{ref,tot}(t) p_i(t), \quad i = 1 \dots N - 1 \\ q_{s,ref,N}(t) &= q_{ref,tot}(t) \left(1 - \sum_{j=1}^{N-1} p_j(t)\right) \end{aligned} \quad (10)$$

In this way, (9) is achieved. The complete model of the four meters machine can be defined as in (11) under the following assumptions:

- All the maximal speeds are fixed to ω_{max} ,
- All the screw gains are considered time invariant ($K_{s,i}(t) = K_{s,i}$),
- All the maximal flow rates are defined as $q_{s,i,max}(t) = q_{s,i,max} = K_{s,i} \omega_{max}$,
- K_p and K_i are considered fixed for all the primary meters,
- $N = 4$, $i = 1 \dots 4$.

Input	Value	Input	Value
ω_{max}	3000 rpm	$\bar{q}_{ref,tot}$	300 kg/h
$K_{s,1}$	0.11900 kg/h/rpm	\bar{p}_1	0.887
$K_{s,2}$	0.07420 kg/h/rpm	\bar{p}_2	0.100
$K_{s,3}$	0.03730 kg/h/rpm	\bar{p}_3	0.010
$K_{s,4}$	0.00698 kg/h/rpm		
τ_1	1 s		
τ_2	2 s		
τ_3	5 s		
τ_4	10 s		

(a) Model parameters

(b) Equilibrium inputs

Table 1: Model parameters and equilibrium inputs

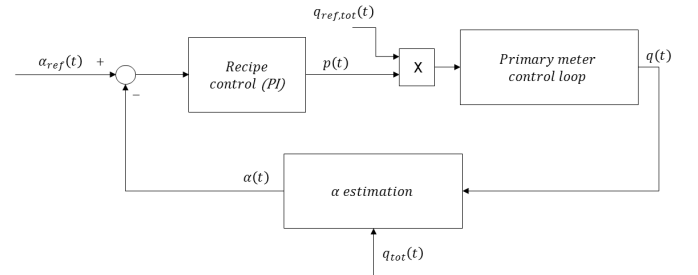


Figure 12: Recipe control scheme

This system is MIMO (Multiple Inputs, Multiple Outputs) with 4 inputs: $q_{ref,tot}(t)$, $p_1(t)$, $p_2(t)$ and $p_3(t)$ and 4 outputs: $\alpha_i(t)$, $i = 1, \dots, 4$. Actually, since the percentage of the fourth ingredient is fully determined by the others, the system has only 3 degrees of freedom, and therefore the problem will be to control $\alpha_i(t)$, $i = 1, \dots, 3$ using $p_i(t)$, $i = 1, \dots, 3$ ($q_{ref,tot}(t)$ is then herein considered as an exogenous disturbance). In order to evaluate the open and closed loop performance, the linearization of this model is carried out around the values in Table 1b. As it can be observed, the dynamics of the different primary meters $\tau_{1..4}$ are changed, with the aim to show the robustness of the controlled system. In order to evaluate the performance of the system, it is possible to observe the transfer functions from $q_{ref,tot}(t)$ to $Y(t)$. Specifically, these subsystems can be defined as:

- $G_q(s) = G(1..3, 1)$ that represents the transfer functions from $q_{ref,tot}(t)$ to $Y(t)$
- $G_a(s) = G(1..3, 2..4)$ that represents the transfer functions from $p_1(t)$, $p_2(t)$ and $p_3(t)$ to $Y(t)$

The recipe control scheme is represented in Figure 12: the transfer function from $q_{ref,tot}(t)$ to $Y(t)$ (usually called sensitivity

$$\left\{ \begin{array}{l}
\frac{dl_i(t)}{dt} = (q_{ref,tot}(t)p_i(t) - q_{s,i}(t)), \quad i = 1 \dots N-1 \\
\frac{dq_{s,i}(t)}{dt} = \frac{1}{\tau_i} (-q_{s,i}(t) + K_{s,i}(K_p(q_{ref,tot}(t)p_i(t) - q_{s,i}(t)) + K_i l_i(t)) \frac{\omega_{max}}{q_{s,i,max}}), \quad i = 1 \dots N-1 \\
\frac{dl_N(t)}{dt} = (q_{ref,tot}(t)(1 - \sum_{j=1}^{N-1} p_j(t)) - q_{s,N}(t)) \\
\frac{dq_{s,N}(t)}{dt} = \frac{1}{\tau_N} (-q_{s,N}(t) + K_{s,N}(K_p(q_{ref,tot}(t)(1 - \sum_{j=1}^{N-1} p_j(t)) - q_{s,N}(t)) + K_i l_N(t)) \frac{\omega_{max}}{q_{s,N,max}}) \\
\alpha_i(t) = \frac{q_{s,i}(t)}{\sum_{j=1}^N q_{s,j}(t)}, \quad i = 1 \dots N-1
\end{array} \right. \quad (11)$$

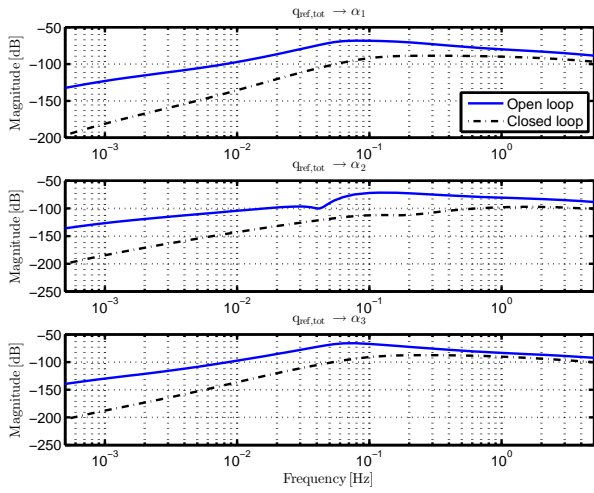


Figure 13: Bode diagrams of the transfer function between $q_{ref,tot}(t)$ and α_i , $i = 1, 2, 3$.

function) is equal to $S(s) = (I - R(s)G_a(s))^{-1}G_q(s)$. In order to define the structure of regulator matrix ($R(s)$: 3 inputs, 3 outputs) the RGA (Relative Gain Array) method is used.

Starting from $G_a(s)$, it is possible to obtain $\Lambda = G_a(0) \odot (G_a(0))^{-1} = I_3$, where I_3 is the 3×3 identity matrix. It means that the system is statically decoupled and is possible to treat the complete MIMO system as 3 SISO (Single Input, Single Output) systems; for this reason a decoupled regulator is employed. The structure of each SISO regulator must guarantee the stability of the system and ensure that $S(s)$ has a magnitude as close as possible to 0. To this purpose, a simple PI regulator provides good performance, as shown in Figure 13. The simulation results, made on a 4 primary meters dosing machine, are represented in Figures 14 and 15 where a step response is shown in terms of $q_{s,i}(t)$ and $\alpha_i(t)$. As it can be seen, this external control loop allows one to obtain a large enhancement of the dosing quality in terms of

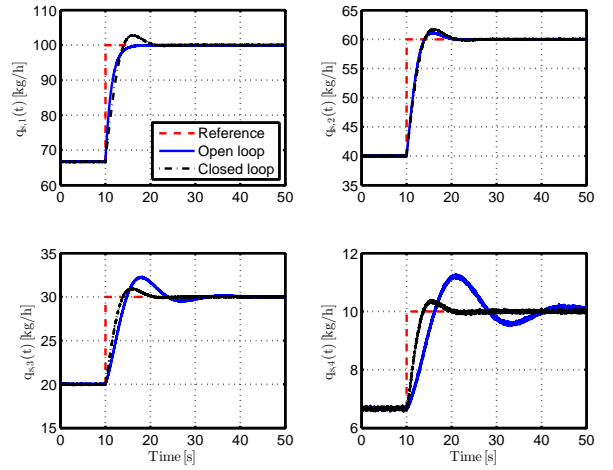


Figure 14: Recipe control: flow rate responses

$q_{ref,tot}$ [kg/h]	$\alpha_{ref,1}$	$\alpha_{ref,2}$	$\alpha_{ref,3}$	Transient time [s]
300	0.887	0.1	0.01	4.7
200	0.5	0.3	0.15	7.6
100	0.4	0.3	0.2	8

Table 2: Recipe control performance.

error amplitude and duration. In order to prove the robustness of this closed loop system some tests are made in different conditions: stability is guaranteed in each configuration and, as can be observed in Table 2, the transient time, with a step variation from $2/3$ of $q_{ref,tot}$ to $q_{ref,tot}$, is always lower than 8 s. Concerning the mixer, a control loop with a simple P controller can be designed in order to avoid undesired emptying of the mixer.

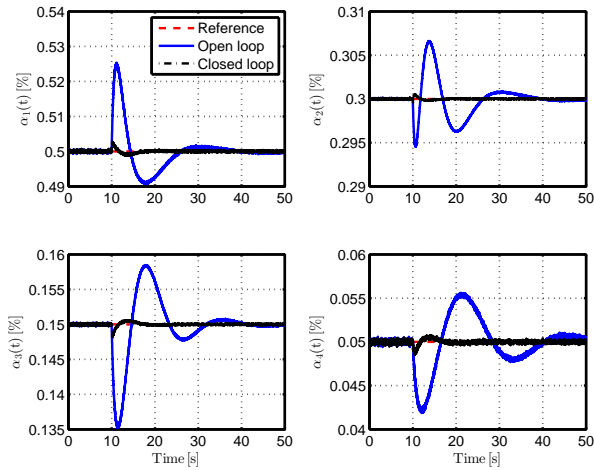


Figure 15: Recipe control: alpha responses

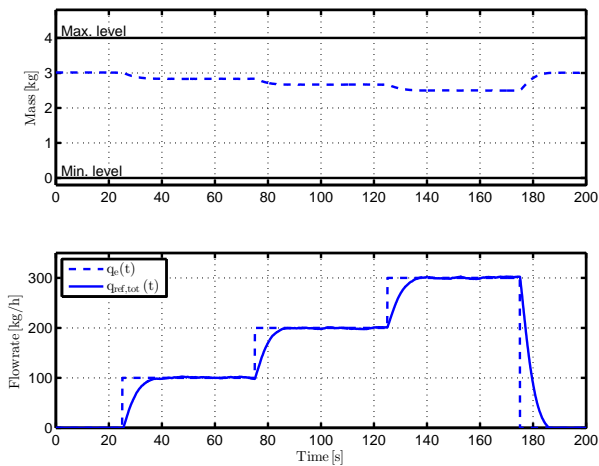


Figure 16: Mixer control

Simulation results are presented in Figure 16. The weight set point $M_{ref}(t)$ is set to 3 kg. The mixer weight is always inside the defined safety range $0 \div 4$ kg and, in steady state, the outgoing flow rate $q_e(t)$ is equal to the reference flow rate $q_{ref,tot}(t)$.

4 CONCLUDING REMARKS

In this paper, a complete architecture for the control of continuous gravimetric blenders in polymer processes has been proposed. The structure of the presented scheme has different layers. The outer one is devoted to avoid the emptying of the mixer, whereas, in the inner one, the recipe is achieved by regulating the percentage of single ingredients with suitable decoupled controllers and the numerical value of the plastic flow rate is computed via extended Kalman filtering. The performance of the

overall scheme has been showed to be effective in a simulation environment. Future work will be devoted to robust and adaptive controller design.

REFERENCES

- [1] Costin, M. H., Taylor, P. A., and D., W. J., 1982. “A critical review of dynamic modelling and control of plasticating extruders”. *Polymer Engineering and Science*, **22**(7), pp. 393–401.
- [2] Costin, M. H., Taylor, P. A., and D., W. J., 1982. “On the dynamics and control of a plasticating extruder”. *Polymer Engineering and Science*, **22**(17), pp. 1095–1106.
- [3] Kochhar, A. K., and Parnaby, J., 1977. “Dynamical modelling and control of plastics extrusion processes”. *Automatica*, **13**, pp. 177–183.
- [4] Fenner, R. T., Cox, A. P. D., and P., I. D., 1979. “On the dynamics and control of a plasticating extruder”. *Surging in screw extruders*, **20**(6), pp. 733–736.
- [5] Mudalamane, R., and Bigio, D. I., 2003. “Process variations and the transient behavior of extruders”. *AIChE Journal*, **49**(12), pp. 3150–3160.
- [6] Rauwendaal, C., 2001. *Polymer Extrusion*. Hanser.
- [7] Broadhead, T., Patterson, W. I., and Dealy, J. M., 1996. “Closed loop viscosity control of reactive extrusion with an in-line rheometer”. *Polymer Engineering and Science*, **36**(23), pp. 2840–2851.
- [8] Chiu, S. H., and Pong, S. H., 2000. “In-line viscosity fuzzy control”. *Journal of Applied Polymer Science*, **79**(7), pp. 1249–1255.
- [9] Del Pilar Noriega, M., and Rauwendaal, C., 2001. *Troubleshooting the extrusion process : a systematic approach to solving plastic extrusion problems*. Hanser.
- [10] Previdi, F., Savaresi, S. M., and Panarotto, A., 2006. “Design of a feedback control system for real time control of flow in a single screw extruder”. *Control Engineering Practice*, **14**, pp. 1111–1121.
- [11] Wellstead, P. E., Health, W. P., and Kjaer, A. P., 1998. “Identification and control of web processes: polymer film extrusion”. *Control Engineering Practice*, **6**, pp. 321–331.
- [12] Isermann, R., and Raab, U., 1993. “Intelligent actuators ways to autonomous actuating systems”. *Automatica*, **29**, pp. 1315–1331.
- [13] Bittanti, S., and Savaresi, S. M., 2000. “On the parametrization and design of an ekf frequency tracker”. *IEEE Trans. on Automatic Control*, **45**(9), pp. 1718–1724.
- [14] Ahrens, J. H., and Khalil, H. K., 2007. “Closed-loop behavior of a class of nonlinear systems under ekf-based control”. *Automatic Control, IEEE Trans. on*, **52**(3), pp. 536–540.
- [15] Schauer, T., Negård, N.-O., Previdi, F., Hunt, K., Fraser, M., Ferchland, E., and Raisch, J., 2005. “Online identification and nonlinear control of the electrically stimulated quadriceps muscle”. *Control Engineering Practice*, **13**(9), pp. 1207–1219.